Drug Development and Industrial Pharmacy, 2010; 36(12): 1404–1412

informa
healthcare

ORIGINAL ARTICLE

Determination of carbamazepine polymorphic contents in double-layered tablets using transmittance- and reflectance-near-infrared spectroscopy involving chemometrics

Makoto Otsuka[1] and Yuya Fukui[2]

[1]*Research Institute of Pharmaceutical Sciences, Faculty of Pharmacy, Musashino University, Nishitokyo, Tokyo, Japan, and* [2]*Department of Pharmaceutical Technology, Kobe Pharmaceutical University, Higashinada, Kobe, Japan*

Abstract

Background: Since polymorphs exhibit differences in chemical and physicochemical stability, characteristics, and dissolution rate of the bulk powder, they may significantly affect on the bioavailability of pharmaceutical compounds. *Aim*: The purpose of the present study is to establish a method for determining the carbamazepine (CBZ) polymorphic content of a double-layered tablet containing various ratios of forms I and III by using transmittance- and reflectance-near-infrared (TNIR and RNIR) spectroscopy involving chemometrics. *Methods*: Both TNIR and RNIR instruments were used to analyze both top (form I) and wire (form III) sides of the compacts, respectively. NIR spectra were analyzed to predict polymorphic content by a principal component regression analysis. NIR data of the tablets were divided into two wavelength ranges: between 860 and 1680 nm (FW), and 1245 and 1285 nm (NW). *Results*: The calibration models for polymorphic content based on TNIR had a linear relationship, but those based on RNIR did not. The accuracy of the calibration models suggested that the double-sided data set is more robust than the single-sided data set. Since the spectra of FW involved various information, the calibration models showed a linear correlation, but it is difficult to understand their model. In contrast, those of NW provided limited information on polymorphic forms making it very easy to understand the model. *Conclusion*: Limiting the wavelength of the spectra is useful to help understand the calibration-complicated model.

Key words: *Carbamazepine polymorph; chemometrics; double-layered tablet; Fourier-transformed near-infrared spectroscopy; principal component regression analysis*

Introduction

Polymorphs exhibit differences in chemical and physicochemical stability, processing characteristics, and dissolution rate, and so on. Particularly, a change in the dissolution rate may significantly affect the drug absorption of the oral dosage form in the gastrointestinal tract resulting in variation in the bioavailability of pharmaceutical compounds[1–5].

Therefore, an accurate assessment of the polymorphisms and solvates of bulk materials is required for the reproducible preparation of pharmaceutical products. Analytical methods for polymorphs include powder X-ray diffraction[6], differential scanning calorimetry (DSC)[7], thermal gravimetric analysis microcalorimetry[8], infrared spectroscopy[9], Raman spectroscopy[10], solid-state NMR[11], and dissolution kinetics[12]. However, they are consuming much time in the preparation of samples and/or measurements. With the introduction of guidelines for process analytical technology (PAT) by the Food and Drug Administration, on-line, real-time analyses as a tool for monitoring and controlling manufacturing processes have become increasingly accepted in the pharmaceutical industry[13–17].

As near-infrared (NIR) spectroscopy[18] involving chemometrics[19] can measure drug and/or polymorphic

Address for correspondence: Makoto Otsuka, Ph.D., Research Institute of Pharmaceutical Sciences, Faculty of Pharmacy, Musashino University, 1-1-20 Shinmachi, Nishitokyo, Tokyo 202-8585, Japan. Tel: +81-424-68-8658, Fax: +81-424-68-8658. E-mail: motsuka@musashino-u.ac.jp

(Received 18 Jun 2009; accepted 10 Apr 2010)

ISSN 0363-9045 print/ISSN 1520-5762 online
DOI: 10.3109/03639045.2010.487262

contents directly on the surface of intact samples without any pretreatment during pharmaceutical manufacturing processes, chemometrical NIR spectroscopic methods have been used to determine the drug content, drug stability[20], tablet coating[21], polymorphic content[22–26], the particle size of powders[27–32], tablet hardness[33–37], and dissolution rate[38].

NIR spectroscopy is rapidly becoming an important technique for PAT in the pharmaceuticals industry. Norris et al.[29] and Otsuka et al.[39] suggested that polymorphic content varied during pharmaceutical processes with physical and chemical conditions such as heat, mechanical stress, and/or the presence of moisture, solvents, and excipients[40].

Previously[24–26], the crystallinity and/or the polymorphic content of the bulk powder of pharmaceuticals have been evaluated using chemometric methods, such as principal component analysis (PCA)/principal component regression (PCR) and partial least squares regression[19]. The results suggested that the crystallinity and/or polymorphic contents of bulk drug powder in a conventional dosage form could be evaluated by the chemometrical NIR method[41–43].

However, there are two types of dosage forms in a current market: one is a conventional tablet in which bulk drug powder is homogenously distributed in the tablet, and the other is a nonconventional tablet in which multidrug is loaded heterogeneously in tablet, to control drug release and stabilization such as dry-coated tablets and multilayered tablets. As mentioned above, the polymorphic content of the dosage forms also varied during pharmaceutical processes[22,39]. It is not easy to measure the polymorphic content of heterogeneous drug-loaded dosage forms by the photospectroscopic method because light dose not penetrate well inside a powder bed of solid-dosage forms.

The purpose of this study is to establish a method for measuring the polymorphic content in a heterogeneous drug-loaded tablet using noncontact and nondestructive methods for PAT. Double-layered tablets[44] containing polymorphic forms of carbamazepine (CBZ)[39,45–47], an anticonvulsive drug, were used as a model. The calibration models to evaluate the polymorphic content of the tablets were investigated using reflectance-NIR (RNIR) and transmittance-NIR (TNIR) spectroscopies involving chemometrics.

Materials and methods

Materials

CBZ bulk powder of Japanese Pharmacopoeia XIII grade (lot No. CEE-9-5) was obtained from Katsura Chem. Co., Tokyo, Japan. The CBZ bulk powder was identified as form I (anhydrate, monoclinic CBZ)[38,47]; form III (anhydride) was obtained by heating dihydrate at 115°C in vacuo for 6 hours. All of the CBZ samples were passed through a No. 200 mesh (75 μm) screen. The X-ray diffraction patterns and the DSC curves of forms I and III CBZ were significantly different and identical to those reported[47].

X-ray powder diffraction analysis

X-ray powder diffraction (XRD) profiles were obtained using an X-ray diffractometer (RINT-ULTIMA, Rigaku Co., Ltd., Tokyo, Japan). The following measurement conditions were included: scan mode—step scan; target—Cu; filter—Ni; voltage—40 kV; current—20 mA; scan speed—2.0° per minute; receiving slit—0.1 mm; time constant—1 second; and scan width—0.1 degree/step.

Thermal analysis

DSC was performed with a Type 3100 instrument (Mac Science Co., Tokyo, Japan). The operating conditions in an open-pan system were as follows: sample weight—5 mg; heating rate—10°C/min; and N_2 gas flow rate—30 mL/min.

Tableting compression process

The manufacturing process for the double-layered tablet (Figure 1) was as follows: one sample (0, 20, 50, 100, 150, 180, and 200 mg of form I) was put into a die 8 mm in diameter and lightly pressed by hand with a flat-surface 8-mm punch in diameter. After removing the punch, the second component (200, 180, 150, 100, 50, 20, and 0 mg of form III) was added into the same die and pressed at 49 MPa with a punch at a compression speed of 15 mm/min with a compression/tension tester (Autograph, Model IS-5000, Shimadzu Co., Kyoto, Japan) at 25 ± 1°C.

Fourier-transformed NIR spectroscopy

RNIR were recorded with a fiberoptic probe of an NIR spectrometer (NH1100, Spectron Tech Co., Soule,

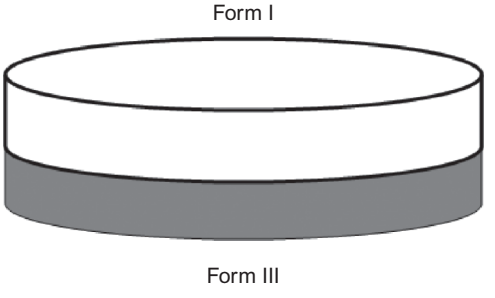

Figure 1. Double-layered tablet (total 200 mg) consisting of forms I and III CBZ.

Korea) with 1.0-mm diameter spot. Detector: photodiode array type, InGaAs, 128 pixels; light source: tungsten halogen lamp. RNIR was measured 32 scans per sample with 2 nm resolution and recorded in the spectral range of 1100–1750 nm. TNIR spectra were taken using an NIR spectrometer (NIRTAB^{TM}, Buchi AG, Flawil, Swaziland). Detector: InGaAs; sample interface: transmission measurement; background reference: Spectralon; resolution: 3 nm; scan number: 32 scan; Fourier processing parameters: apodization function, rectangular. TNIR was recorded in the spectral range of 860–1660 nm with 10 mm in diameter spot.

NIR spectra of 35 sample tablets (7 polymorphic concentration levels, 5 tablets each) were recorded from the top (form I) and the wire (form III) sides of the tablet with both TNIR and RNIR spectrometers, respectively. All of spectra were transformed into absorbance and area normalization as pretreatment. The 42 NIR spectra of the top and the wire of 21 tablets were used as a calibration dataset to establish a model to predict polymorphic content by PCR analysis. The 28 spectra of the top and the wire sides of the other 14 tablets were used as a validation dataset to validate the calibration model.

In the multivariate data analysis[19], to predict value y from a suite of other measurement x_j (where $j = 1, 2,\ldots, y = m$), we must first establish a relationship between the two sets of measurements. If we assume that y is linearly related to x and write

$$y = \beta_0 + \beta_1 x_1 + \beta_2 x_2 + \cdots + \beta_m x_m + f, \tag{1}$$

then the β specifies the relationship, and f contains the error in describing this relationship. For a set of n samples ($i = 1, 2,\ldots, n$):

$$y_i = \beta_0 + \beta_1 x_{i1} + \beta_2 x_{i2} + \cdots + \beta_m x_{im} + f_i. \tag{2}$$

In matrix format, this becomes

$$\mathbf{y} = \mathbf{X}\boldsymbol{\beta} + \mathbf{f}.$$

The error vector, **f**, is included because it is unlikely that **y** can be expressed exactly in terms of the **X** block; $\mathbf{f}_i$ is the **y** residual for the ith sample. The determination of the vector of regression coefficients allows future values to be predicted from future **X** block measurements. Thus, finding the $\boldsymbol{\beta}$ vector is described as creating a regression model.

PCR is presented as regression of **y** on selected principal components (PCs) of **X**. Properties of PCR are given together with a discussion on selection of eigenvectors.

A spectrum including n spectral data can be seen as a point in an n-dimensional space. In multivariate data analysis, PCA/PCR of a spectral data matrix **X** is a basic tool. PCA/PCR decomposes **X** into three matrices (Equation 3):

$$\mathbf{X} = \mathbf{USV}^{\mathrm{T}}. \tag{3}$$

This decomposition is particularly useful for converting **X** into a few information plots (score plots and loading plots) and for modeling the systematic structure in **X**. The **U** matrix holds the eigenvectors of the row space, the **V** matrix holds eigenvectors of the column space, **S** is a diagonal matrix whose diagonal elements are the singular values, **T** is a scores matrix, and **L** is a loadings matrix.

$$\mathbf{L} \equiv \mathbf{V}, \tag{4}$$

$$\mathbf{T} \equiv \mathbf{US}, \tag{5}$$

$$\mathbf{y} = (\mathbf{USV}^{\mathrm{T}})\boldsymbol{\beta} + \mathbf{f}. \tag{6}$$

The solution then becomes

$$\boldsymbol{\beta} = \mathbf{VS}^{-1}\mathbf{U}^{\mathrm{T}}\mathbf{y}, \tag{7}$$

where $\boldsymbol{\beta}$ is the regression vector. Predicting **y** from a new **x** form from

$$\mathbf{y}_{\mathrm{new}} = \mathbf{x}_{\mathrm{new}}\boldsymbol{\beta} = \mathbf{x}_{\mathrm{new}}\mathbf{VS}^{-1}\mathbf{U}^{\mathrm{T}}\mathbf{y}. \tag{8}$$

The chemometric analysis was performed using the PCR program associated with the Pirouette software (InfoMetrix Co., Woodenville, WA, USA). The best conditions of the calibration model were determined based on the NIR spectra calibration dataset to minimize the SE of cross-validation (SECV) by the leave-one-out method. The obtained calibration model was validated based on a validation dataset.

Results and discussion

Characterization of CBZ polymorphic forms by XRD and DSC

Polymorphic forms I and III of CBZ prepared in accord with the published methods[38,39] were characterized by

XRD and DSC measurements. The XRD profile of form I had three diffraction peaks at $2\theta^\circ$ = 13.0°, 14.1°, and 17.0°, and that of form III had at $2\theta^\circ$ = 12.0° and 19.6°. The DSC curve of the form I showed endothermic and exothermic peaks at around 170°C due to melting of form I and crystal growth of form III, after then an endothermic peak at 195°C due to melting of form III. On the contrary, the DSC curve of form III had only an endothermic peak at 195°C due to melting as reported previously[32,33]. The results of XRD and DSC of both crystalline CBZ forms were significantly different and identical to those reported[32,33]. After compression at 49 MPa, the XRD profiles of forms I and III were unchanged because the crystalline transformation of either form was not induced under the compression conditions. Therefore, polymorphic content of forms I and III in the double-layered tablets was not changed.

NIR spectra of double-layered tablets containing CBZ polymorphs

Figure 2 showed the TNIR and RNIR spectra of forms I and III CBZ, and those were significantly different and identical to those reported. In the TNIR spectra, NIR spectral peaks were assigned based on the data[48] as follows, the peak at 876 nm is attributable to the third over tone C–H stretching, that at 1015 nm to N–H stretching of $CONH_2$ (Structure 1), that at 1100–1140 nm to a combination of second over tone C–H stretching and second over tone C=C stretching of the benzene ring, those at 1190 and 1257 nm to second over tone C–H stretching and those at 1465 and 1517 nm to first over tone N–H stretching of CONH. In the RNIR spectra, NIR spectral peaks were also assigned as follows[48], the peak at 1130 nm is attributable to second over tone C–H stretching, those at 1468 and 1515 nm to first over tone N–H stretching of $CONH_2$ and that at 1680 nm to first over tone C–H stretching of the benzene ring. As shown in Figure 2, the bands attributable to second over tone C–H stretching, first over tone N–H stretching of $CONH_2$, and first over tone C–H stretching of the benzene ring were observed in RNIR, but did not in TNIR, because the baseline of TNIR at wavelength region between 1400 and 1700 nm was over 6, and saturated.

Both the top and the wire sides of double-layered tablets containing various ratio of forms I and III were measured by RNIR and TNIR, respectively. Figures 3 and 4 show TNIR and RNIR spectra of the top of the tablets. As shown in Figure 3, the order of the TNIR peak intensity of the sample tablet followed that of the polymorphic content of the tablet, but the RNIR intensity in Figure 4 did not. The order of the peak intensity of TNIR for the top was almost the same as that for the wire side, but that of RNIR for the top side was different from that for the wire. These results suggested that TNIR spectra could provide information on polymorphic content for a whole tablet, but RNIR spectra could not, because the

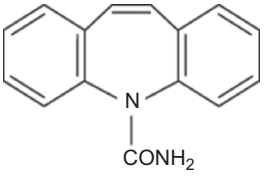

Structure 1.

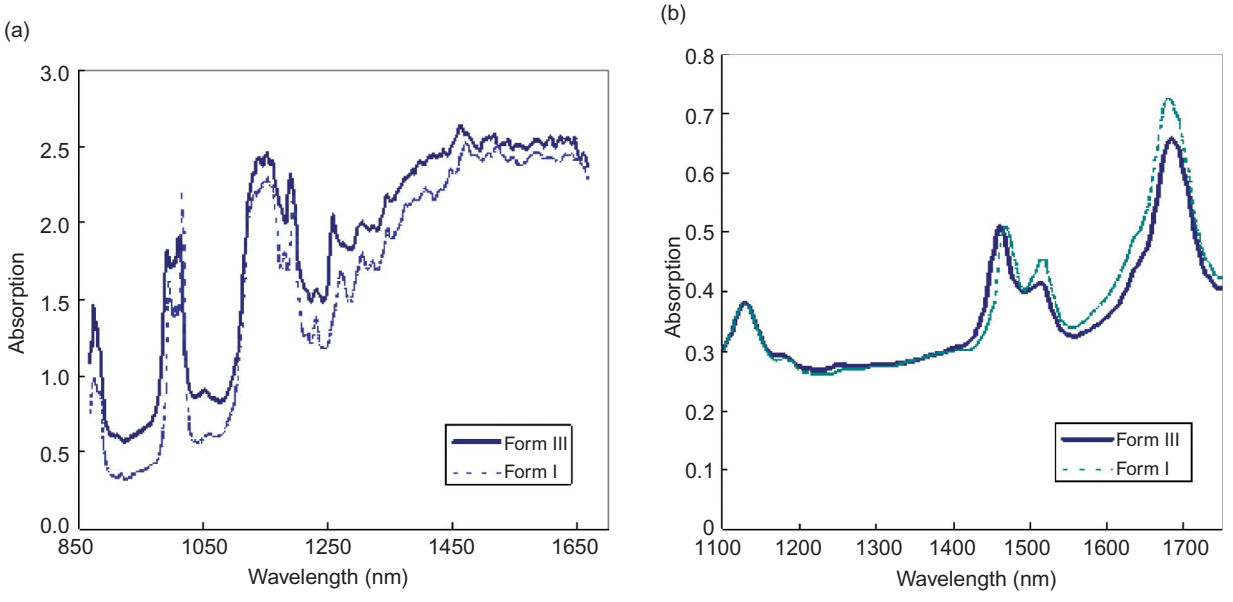

Figure 2. TNIR (a) and RNIR (b) spectra of forms I and III CBZ.

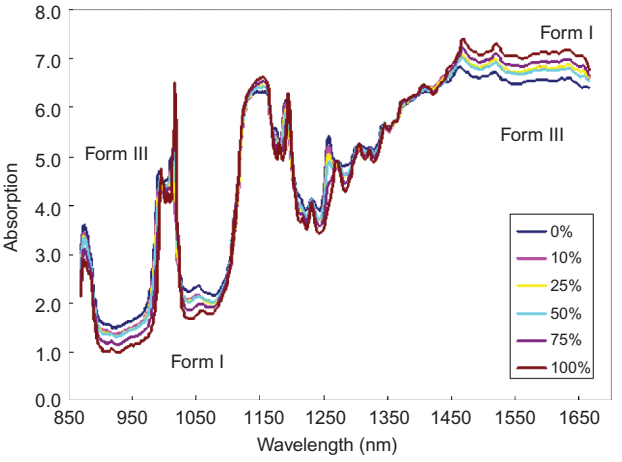

Figure 3. TNIR spectra of double-layered tablets consisting of various ratios of forms I and III CBZ (0:100, 10:90, 25:75, 50:50, 75:25, 90:10, and 100:0).

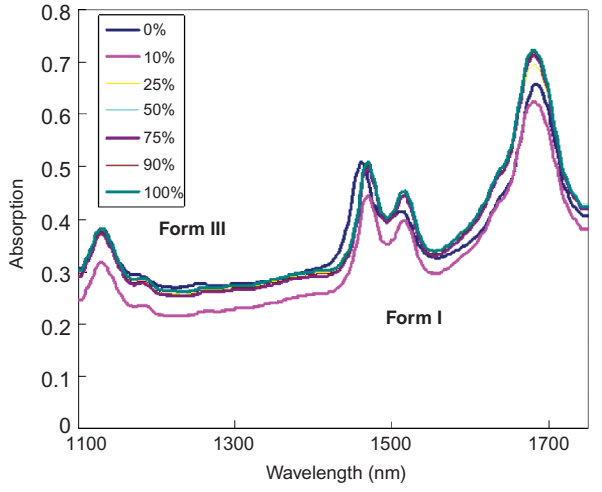

Figure 4. RNIR spectra of double-layered tablets consisting of various ratios of forms I and III CBZ.

reflecting light had not reached deep enough in the case of RNIR.

Chemoinformetric NIR spectroscopy

Chemometrics can be used to decompose raw data profiles and help us to understand the significant contribution of a specific group's data. In this section, to predict polymorphic content of the heterogeneous drug-loaded dosage forms, calibration models were established based on TNIR and RNIR spectra of the double-layered tablets by PCR.

The calibration models established based on TNIR had a linear relationship. However, the model based on RNIR did not because the reflecting light might not have reached deep enough. Gottfries et al.[49] reported that the drug content of metroprolol tablets could be measured by TNIR and RNIR. Cournoyer et al.[50] reported that drug concentration in tablet measured three different NIR instruments and compared each other. They concluded that TNIR was more accurate than RNIR. Their results were consistent with the present results.

To clarify the scientific evidence of the calibration model, the TNIR datasets of the tablets were divided into two wavelength ranges between 860 and 1680 nm (FW) and 1245 and 1285 nm (NW). The calibration models were then recalculated based on the datasets of limited wavelength regions by PCR after transformed area normalization as pretreatment and are summarized in Tables 1 and 2. The peak intensity of TNIR spectra datasets in all wavelength ranges followed polymorphic contents. Peak area-normalized TNIR spectra for the top of the tablets with wavelength ranges of NW are shown in Figure 5 as an example. In NW, the peak at 1257 nm decreased, and that at 1270 nm increased with an isosbestic point, clearly indicating a change of polymorphic content of forms I and III due to the second over tone C–H stretching. The SECV calculated based on TNIR datasets for the top and the wire sides of FW and NW were summarized in Table 1. The % variance and SECV of the first PC (PC1) calculated based on FW dataset were 88.2%, 12.271 and those of the second PC (PC2) were 6.07% and 3.30, respectively. In contrast, those of PC1 based on NW were 99.5% and 5.11. The result indicated that the calibration models for both sides in FW and NW consisted of two and one PC, respectively. Because the FW spectra contained a lot of chemical, physicochemical, and physical information such as drug content, polymorph, and particle size, the dataset had multi-isosbestic points on the spectra, but

Table 1. The % Variance and standard error of cross validation (SECV) calculated based on TNIR data sets for the top and the wire sides of FW and NW.

	FW		NW	
	% Variance	SECV	% Variance	SECV
PC1	88.213	12.371	99.105	5.110*
PC2	6.070	3.301*	0.556	5.162
PC3	1.755	3.315	0.098	5.234
PC4	0.611	3.239	0.060	5.260

*: the lowest value.

Table 2. The multiple correlation coefficients (γ^2) and standard error of calibration (SEC) and number of principal components (PC) for various calibration models.

	Double sides			Top side			Wire side		
	SEC	γ^2	PC	SEC	γ^2	PC	SEC	γ^2	PC
FW	3.253	0.9962	2	3.281	0.9965	3	2.537	0.9978	2
NW	5.055	0.9908	1	5.397	0.9898	1	4.003	0.9944	1

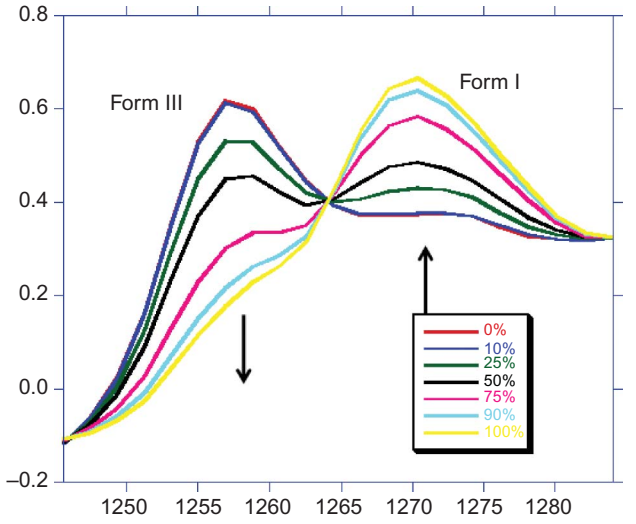

Figure 5. Limited-TNIR spectra in NW of double-layered tablets consisting of various ratios of forms I and III CBZ (0:100, 10:90, 25:75, 50:50, 75:25, 90:10, and 100:0).

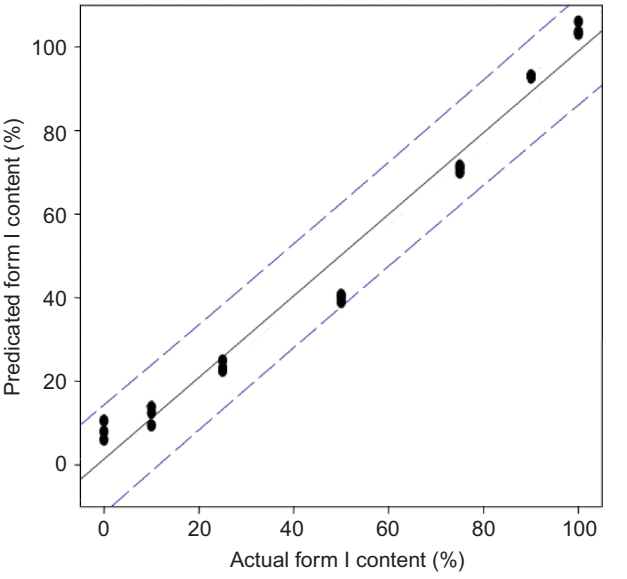

Figure 6. Correlation between actual and predict polymorphic content of double-layered tablets containing forms I and III based on NW of NIR spectroscopy. The symbols and error bars represent the average and SD ($n = 3$). The solid line and long dashed line represent the regression line, 95% predicted interval.

that of NW had an isosbestic point, and the calibration model of FW might be more complex than that obtained with a narrow wavelength range. As NW spectra had limited information concerning polymorphic form, the calibration model is simple and easily understood. The result indicated that wavelength range affected the calibration model structure.

Table 2 shows the multiple correlation coefficients (γ^2) and standard error of calibration (SEC) for various calibration models. The γ^2 of the wire side of FW was the highest value, 0.9978, and that of the double sides of NW was the lowest, 0.9906. The SEC of the wire side of FW was the lowest, 2.537, and that of the top side was the highest, 5.397. The γ^2 of the calibration model of FW is larger than that of NW, but the SEC is smaller than that of NW. Since the spectra data of wavelength range contained chemical, physicochemical, and physical information, the calibration model might be more complex. Therefore, it is possible to measure more accurately parameters based on more complicated datasets, but it is not so easy to clarify the scientific evidence of the complicated model to measure an objective function. The relationship between the predicted and actual polymorphic content of all datasets for the top and/or the wire sides of tablets for FW and NW gives a straight line, respectively. The relationship for NW is shown in Figure 6 as an example, the predicted value at 50% was relatively lower, but the whole plot gives a reasonable straight line, with a slope of 0.9801, a Y-intercept of 1.065, and γ^2=0.9809. These predicted values were all within the 95% predictive intervals, indicating that TNIR has good predictive potential for polymorphic content in double-layered tablets.

Accuracy of the calibration models for polymorphic content of double-layered tablets

To evaluate the accuracy of calibration model, the polymorphic content of the double-layered tablets was evaluated based on various kinds of validation datasets for the tablets. The calibration models were obtained based on the calibration datasets for FW and NW of the top and/or the wire of tablets, and the predicted values were obtained to evaluate based on the validation datasets. The accuracy (Am) and bias (Bm) of the calibration models were calculated based on the predicted values using Equation 10 and are summarized in Table 3.

Table 3. Validation results of the calibration models for FW and NW of the top and/or the wire of tablets.

		FW			NW		
Calibration	Validation	PC	SEV	Am (%)	PC	SEV	Am (%)
Both sides	Both sides	2	3.301	6.127	1	5.110	7.711
Both sides	Top side	2	3.301	5.906	1	5.110	6.884*
Both sides	Wire side	2	3.301	4.517	1	5.110	8.538
Top side	Both sides	3	3.349	5.877	1	5.523	8.689
Top side	Top side	3	3.349	4.517*	1	5.523	6.894
Top side	Wire side	3	3.349	4.517*	1	5.523	10.485**
Wire side	Both sides	2	2.666*	6.332	1	4.075	8.078
Wire side	Top side	2	2.666*	4.517*	1	4.075	8.63
Wire side	Wire side	2	2.666*	9.522**	1	4.075	7.525

*: the lowest value; **: the highest value.

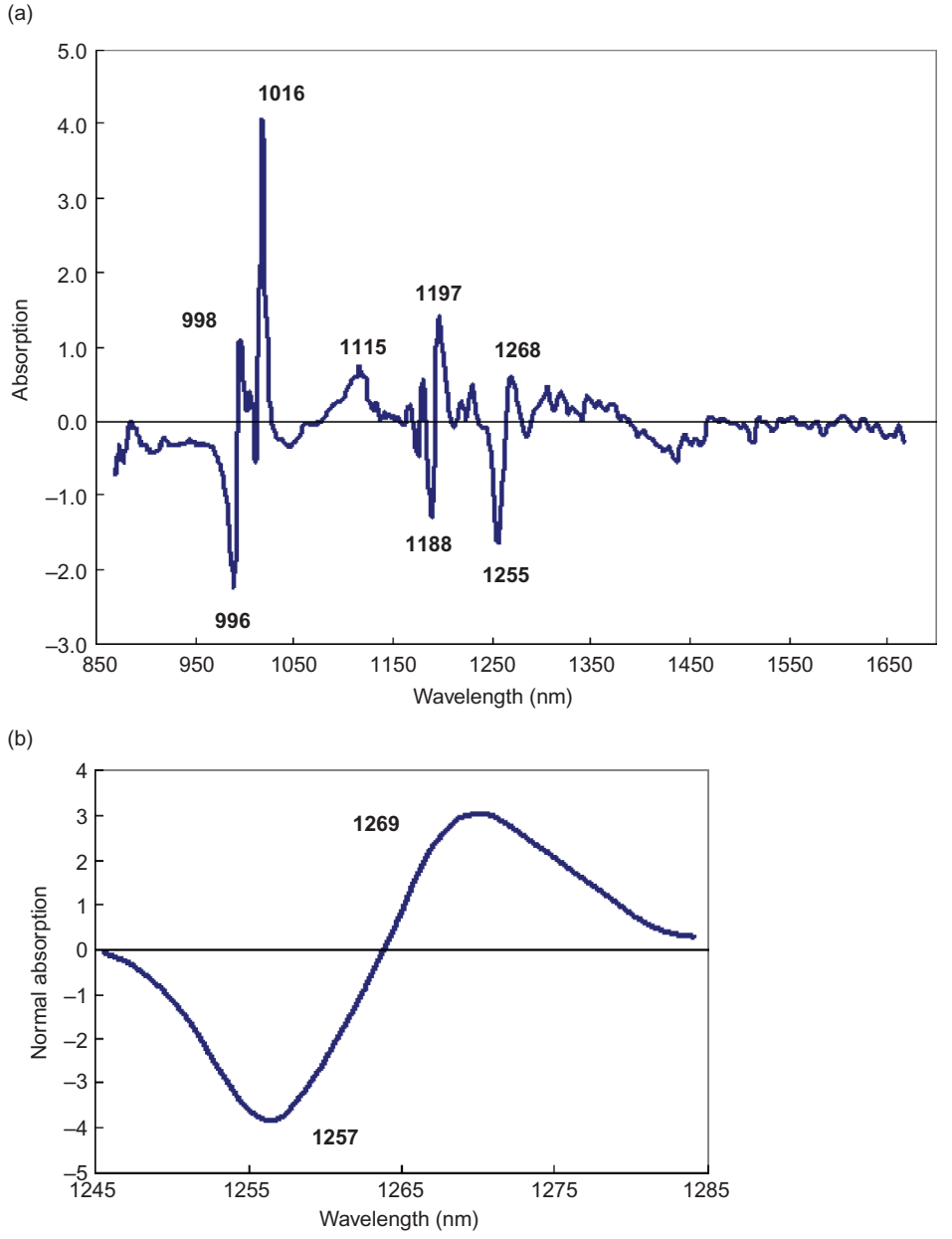

Figure 7. Regression vectors for the calibration models to predict polymorphic content of double-layered tablets consisting of various ratios of forms I and III CBZ based on the spectra in FW (a) and NW (b).

$$A_m = \frac{\sum_{i=1}^{n} \frac{|X_c - X_t|}{X_t}}{n} \times 100. \quad (9)$$

A_m is the percentage mean accuracy, X_c the predicted value of content of form I, X_t the actual value of content of form I, and n the number of experiments.

In FW, Nos. 5, 6, and 8 were the lowest A_ms and No. 9 was the highest. In NW, Nos. 2 and 6 were the lowest and the highest A_ms. Most A_m values were smaller for FW than NW. The A_m of the single-sided set was smaller than that of the two-sided set, but analytical data of the two-sided model were much important because double-layered tablets must measure random tablet surface in practical manufacturing process. This result suggested the double-sided sample set to be more robust than the single-sided dataset. Polymorphic crystalline forms had different characteristics due to crystalline structure, crystal habit, surface morphology, density, and particle

size[1,2]. The powder bed of polymorphic crystalline forms in the tablet had different geometrical structure due to powder flow and compactivity due to particle characteristics[1,2]. Therefore, the polymorphic crystalline forms differenced photometric characteristics, such as absorbance, refraction, and reflection. Because the calibration model of the two-sided datasets involved variability in both polymorphic characteristics, it was more robust.

Scientific evidence of the calibration model to measure polymorphic content of double-layered tablets

As mentioned above, the calibration models of FW and NW to estimate the predicted polymorphic content in the double-layered tablet in Figure 6 were significantly ($P < 0.05$) by multiple regression analysis. A regression vector of the calibration models reflects the scientific evidence of parameters[18,37]. Figure 7 shows the regression vector of the calibration models for FW and NW, respectively. In Figure 7a (FW), the main positive peaks at 998 and 1016 nm are attributable to N–H stretching of $CONH_2$, those at 1115 nm to a combination of second over tone C–H stretching and second over tone C=C stretching of the benzene ring, and those at 1197 and 1268 nm to second over tone C–H stretching[48]. The main negative peak at 994 nm is attributable to the third over tone C–H stretching, and those at 1188 and 1255 nm to second over tone C–H stretching[48]. As shown in Figure 2a, the positive peaks might be due to form I and the negative peaks to form III. However, there are many unknown positive and negative peaks in the regression vectors. In contrast in Figure 7b (NW), there are only two positive and negative peaks at 1257 and 1269 nm due to forms III and I attributable to the second over tone C–H stretching[48] as shown in Figure 2a. Because the spectra of FW involved various information, there are too many positive and negative peaks to explain their role in the regression vector, but those of NW are limited to the second over tone C–H stretching of forms I and III, making it very easy to understand the model, and evaluate the polymorphic content of double-layered tablets.

Conclusions

Because the polymorphic content of CBZ tablets could be evaluated by TNIR spectroscopy with chemometrics, but it could not be by RNIR, the quantitative evaluation of the tablet sample by TNIR was proven to be superior than that by RNIR. Limiting of wavelength range of TNIR spectral datasets is useful to help understand the calibration model and how to evaluate objective functions, but the processing loses important information. These results suggested that the TNIR method provides a rapid quantitative analysis of the polymorphic content of heterogeneous drug loaded-dosage form during preparation processes, as characterized by the simple, nondestructive, and high-sensitive nature of the method.

Acknowledgments

The authors thank Mr. Yukihiro Ohsaka, Kobe Pharmaceutical University for his experimental assistance.

Declaration of interest

This work was supported in part by a grant-in-aid for Scientific Research (Scientific Research, C, No. 17500322) and MEXT HAITEKU (2004–2008) from the Ministry of Education, Culture, Sports, Sciences and Technology, Japan. The authors report no conflicts of interest. The authors alone are responsible for the content and writing of this paper.

References

1. FDA Papers. (1985). Guidelines: Manufacturing and controls for INDs and NDAs, Pharm Tech Japan, 1:835–50.
2. Haleblian JK. (1975). Characterization of habits and crystalline modification of solids and their pharmaceutical applications. J Pharm Sci, 64:1269–88.
3. Otsuka M, Matsuda Y. (1995), Polymorphism, pharmaceutical aspects. In: Swarbrick J, Boylan JC, eds. Encyclopedia of pharmaceutical technology, vol. 12. New York: Marcel Dekker, 305–26.
4. Garg A, Singh S, Rao VU, Bindu K, Balasubramaniam J. (2009). Solid state interaction of raloxifene HCl with different hydrophilic carriers during co-grinding and its effect on dissolution rate. Drug Dev Ind Pharm, 35(4):455–70.
5. Umeda Y, Fukami T, Furuishi T, Suzuki T, Tanjoh K, Tomono K. (2009). Characterization of multicomponent crystal formed between indomethacin and lidocaine. Drug Dev Ind Pharm, 5(7):843–51.
6. Yoshino H, Hagiwara Y, Kobayashi S, Samejima M. (1984). Estimation of polymorphic transformation degree of pharmaceutical raw materials. Chem Pharm Bull, 32:1523–36.
7. Kaneniwa N, Otsuka M, Hayashi T. (1985). Physicochemical characterization of indomethacin polymorphs and the transformation kinetics in ethanol. Chem Pharm Bull, 33: 3447–55.
8. Ahmed H, Buckton G, Rawlins DA. (1996). The use of isothermal microcalorimetry in the study of small degree of amorphous content of a hydrophobic powder. Int J Pharm, 130:195–201.
9. Black DB, Lovering EG. (1977). Estimation of the degree of crystallinity in digoxin by X-ray and infrared methods. J Pharm Pharmacol, 29:684–7.
10. Taylor LS, Zografi G. (1998). The quantitative analysis of crystallinity using FT-Raman spectroscopy. Pharm Res, 15:755–61.

11. Liu J, Nagapudi K, Kiang YH, Martinez E, Jona J. (2009). Quantification of compaction-induced crystallinity reduction of a pharmaceutical solid using (19)F solid-state NMR and powder X-ray diffraction. Drug Dev Ind Pharm, 9:1–7.
12. Berridge JC, Jones P, Roberts-McIntosh AS. (1991). Chemometrics in pharmaceutical analysis. J Pharm Biomed Anal, 9:597–604.
13. Porter SC, Felton LA. (2010). Techniques to assess film coatings and evaluate film-coated products. Drug Dev Ind Pharm, 36(2):128–42. (Review)
14. Müller J, Knop K, Thies J, Uerpmann C, Kleinebudde P. (2010). Feasibility of Raman spectroscopy as PAT tool in active coating. Drug Dev Ind Pharm, 36(2):234–43.
15. Kuentz M, Rothenhäusler B, Röthlisberger D. (2006). Time domain 1H NMR as a new method to monitor softening of gelatin and HPMC capsule shells. Drug Dev Ind Pharm, 32(10):1165–73.
16. Paulson W, ed. (2002). Regulatory Leeway sought for process analytical technology. The Gold Sheet, vol. 36. Chevy Chase, MD: Elsevier.
17. Process Analytical Technology (PAT) Initiative, U.S. Food and Drug Administration Center for Drug Evaluation and Research Home Page. http://www.fda.gov/AboutFDA/CentersOffices/CDER/ucm088843.htm (May 13, 2010).
18. Siesler W, Ozaki Y, Kawano S, Heise HM. (2001). Near-infrared spectroscopy: Principles, instruments, applications. Weinheim: Wiley-VCH.
19. Martents H, Næs T. (1989). Multivariate calibration. New York: John Wiley & Sons.
20. Drennen JK, Lodder RA. (1990). Nondestructive near-infrared analysis of intact tablets for determination of degradation products. J Pharm Sci, 79:622–7.
21. Buchanan BR, Baxter MA, Chen TS, Qin XZ, Robinson PA. (1996). Use of near-infrared spectroscopy to evaluate an active in a film coated tablet. Pharm Res, 13:616–21.
22. Norris T, Aldridge PK, Sekulic SS. (1997). Determination of end-points for polymorph conversions of crystalline organic compounds using on-line near-infrared spectroscopy. Analyst, 122:549–52.
23. Patl AD, Luner PE, Kemper MS. (2000). Quantitative analysis of polymorphs in binary and multi-component powder mixtures by near-infrared reflectance spectroscopy. Int J Pharm, 206:63–74.
24. Otsuka M, Kato F, Matsuda Y. (2000). Comparative evaluation of the degree of indomethacin crystallinity by chemoinformetrical fourier-transformed near-infrared spectroscopy and conventional powder X-ray diffractometry. AAPS Pharmsci, 2(1): Article 9. http://www.pharmsci.org/ [accessed May 25, 2010].
25. Otsuka M, Kato F, Matsuda Y. (2001). Determination of indomethacin polymorphic contents by chemometric near-infrared spectroscopy and conventional powder X-ray diffractometry. Analyst, 126:1578–82.
26. Fukui Y, Otsuka M. (2010). Determination of the crystallinity of cephalexin in pharmaceutical formulations by chemometrical near-infrared spectroscopy. Drug Devel Ind Pharm, 36(1):72–80.
27. Bull CR. (1991). Compensation for particle size effects in near infrared reflectance. Analyst, 116:781–6.
28. Aucott LS Garthwaite PH. (1988). Transformations to reduce the effect of particle size in near-infrared spectra. Analyst, 113:18491–54.
29. Norris KH, Williams PC. (1984). Optimization of mathematical treatments of raw near-infrared signal in the measurement of protein in hard red spring wheat, I. Influence of particle size. Cereal Chem, 61:158–65.
30. Franke P, Gill I, Luscombe CN, Rudd DR, Waterhouse J, Jayasooriya A. (1998). Near-infrared mass median particle size determination of lactose monohydrate: Evaluating several chemometric approaches. Analyst, 123:2043–6.
31. Otsuka M, Mouri Y, Matsuda Y. (2003). Chemometric evaluation of pharmaceutical properties of antipyrine granules by near-infrared spectroscopy. AAPS PharmSciTech, 4(3):Article 47, 334–40. http://www.pharmascitech.org (May 13, 2010).
32. Otsuka M. (2004). Comparative particle size determination of phenacetin bulk powder by using Kubelka–Munk theory and principle component regression analysis based on near-infrared spectroscopy, Powder Tech, 141:244–50.
33. Morisseau K, Rhodes CT. (1997). Near-infrared spectroscopy as a nondestructive alternative to conventional tablet hardness testing. Pharm Res, 14:108–11.
34. Kirsch JD, Drennen JK. (1999). Nondestructive tablet hardness testing by near-infrared spectroscopy: A new and robust spectral best-fit algorism. J Pharm Biomed Anal, 19: 351–62.
35. Ebube NK, Thosar SS, Roberts RA, Kemper MS, Rubnovitz R, Martin DL, et al. (1999). Application of near-infrared spectroscopy for nondestructive analysis of Avicel powders and tablets. Pharm Dev Technol, 4:19–26.
36. Chen Y, Thosar SS, Forbess RA, Kemper MS, Rubinovitz RL, Shukla AJ. (2001). Prediction of drug content and hardness of intact tablets using artificial neural network and near-infrared spectroscopy. Drug Dev Ind Pharm, 27:623–31.
37. Otsuka M, Yamane I. (2006). Prediction of tablet hardness based on near infrared spectra of raw mixed powders by chemometrics. J Pharm Sci, 95:1425–33.
38. Kahela P, Aaltonen R, Lewing E, Anttila M, Kristoffersson E. (1983). Pharmacokinetics and dissolution of two crystalline forms of carbamzepine. Int J Pharm, 14:103–20.
39. Otsuka M, Hasegawa H, Matsuda Y. (1999). Effect of polymorphic forms of bulk powders on pharamcetutical properties of carbamazepine granules. Chem Pharm Bull, 47:852–6.
40. Radtke G, Knop K, Lippold BC. (2006). Important parameters for the manufacture of slow-release matrix pellets with an aqueous dispersion of quaternary poly(meth)acrylates in the rotary fluidized bed. Drug Dev Ind Pharm, 32(3):287–96.
41. Otsuka E, Abe H, Aburada M, Otsuka M. (2010). Nondestructive prediction of the drug content of an aspirin suppository by near-infrared spectroscopy. Drug Dev Ind Pharm, March 24.
42. Gabrielsson J, Sjöström M, Lindberg NO, Pihl AC, Lundstedt T. (2006). Robustness testing of a tablet formulation using multivariate design. Drug Dev Ind Pharm, 32(3):297–307.
43. Gabrielsson J, Sjöström M, Lindberg NO, Pihl AC, Lundstedt T. (2006). Multivariate methods in the development of a new tablet formulation: Excipient mixtures and principal properties. Drug Dev Ind Pharm, 32(1):7–20.
44. Tian L, Zhang Y, Tang X. (2008). Sustained-release pellets prepared by combination of wax matrices and double-layer coatings for extremely water-soluble drugs. Drug Dev Ind Pharm, 34(6):569–76.
45. Kelmann RG, Kuminek G, Teixeira HF, Koester LS. (2008). Preliminary study on the development of nanoemulsions for carbamazepine intravenous delivery: An investigation of drug polymorphic transition. Drug Dev Ind Pharm, 34(1):53–58.
46. Patterson JE, James MB, Forster AH, Rades T. (2008). Melt extrusion and spray drying of carbamazepine and dipyridamole with polyvinylpyrrolidone/vinyl acetate copolymers. Drug Dev Ind Pharm, 34(1):95–106.
47. Kaneniwa N, Yamaguchi T, Watari N, Otsuka M. (1984). Hygroscopicity of carbamazepine crystalline powders. Yakugaku Zasshi, 104:184–90.
48. Iwamoto M, Kawano S, Uozumi J. (1994), Introduction of near infrared spectroscopy. Tokyo: Sachi Syobou Co.
49. Gottfries J, Depui H, Fransson M, Jongeneelen M, Josefson M, Langkilde FW, et al. (1996). Vibrational spectroscopy for the assessment of active substance in metoprolol tablets: A comparison between transmission and diffuse reflectance near-infrared spectrometry. J Pharm Biomed Anal, 14:1495–503.
50. Cournoyer A, Simard JS, Cartilier L, Abatzoglou N. (2008). Quality control of multi-component, intact pharmaceutical tablets with three different near-infrared apparatuses. Pharm Dev Technol, 13(5):333–43.